

Identification of Physical Parameters of a Synchronous Generator From Online Measurements

M. Karrari and O. P. Malik, *Life Fellow, IEEE*

Abstract—A new method to determine physical parameters of a synchronous generator based on an online measurement of the electrical power, terminal voltage, and field voltage, following a small perturbation of the field voltage, and the rotor angle at the same steady-state operating condition is described in this paper. A multivariable linear transfer function, identified using the sampled input-output data, is converted to the parameters of the Heffron-Phillips model. Using the relations of the Heffron-Phillips parameters with the physical parameters, the physical parameters are estimated. These estimated parameters are then used in a nonlinear structure to model the synchronous generator. Experimental results with the proposed method applied to a micromachine show good accuracy of the model and also show that the identified nonlinear model is valid at other operating conditions. At dramatically different operating conditions, however, to include the effects of unstructured nonlinearities such as magnetic saturation, the parameters of the nonlinear structure can be slightly adjusted for better performance.

Index Terms—Parameter estimation, power system identification, power system modeling, synchronous generators.

I. INTRODUCTION

As power systems become more interconnected and complicated, analysis of dynamic performance of such systems becomes more important. Synchronous generators play a very important role in the stability of power systems. A valid model for synchronous generators is essential for a valid analysis of stability and dynamic performance. Almost three quarters of a century, after the first publications in modeling synchronous generators [1], [2], the subject is still a challenging and attractive research topic.

The first and traditional methods of modeling of synchronous generators are well specified in IEEE standards [3]. These methods assume a known structure for the synchronous machine, using well-established theories like Park transformation. They address the problem of finding the parameters of the known structure (which are called physical parameters in this paper). Usually the procedures involve difficult and time-consuming tests. These approaches include short-circuit tests, standstill frequency response (SSFR) and open circuit frequency response (OCFR). These tests can mainly be carried

out when the machine is not in service. The traditional methods do not take into account the parameter deviations due to changes in loads and other parameters such as temperature.

In modeling synchronous generators, there are two kinds of nonlinearities. The first kind of nonlinearities (structured), are those which are modeled in the well-known nonlinear structures of synchronous models. One example is the sine and cosine functions of the rotor angle. The second kind of nonlinearities (unstructured), are those which are not usually considered in the structure of the models. One example is the magnetic saturation in the iron parts of the rotor and stator. Although some attempts have been made to define some model structures for magnetic saturation [4]–[6], the derived models can hardly show all the realities, as the saturation curves also depend on the operating conditions. The fact is that there is no unique nonlinear structure to define all the system behavior when dealing with a practical synchronous generator with dramatic changes in the operating conditions. The unstructured nonlinearities can be considered by adjusting the physical parameters of the nonlinear model using online measurements.

To overcome the shortcomings of the traditional methods, and, to some extent, include unstructured nonlinearities, online identification methods have been suggested [7]–[20]. These papers can be divided into two categories. Papers in the first category [7], [8], deal with black-box modeling of synchronous generators using input-output data. In these papers the structure of the model is not assumed to be known *a priori* and no physical parameters are estimated. Their only concern is to map the input data set to the output data set.

The second category [9]–[20] of papers assumes a known structure for the synchronous machine (as the traditional methods), and tries to estimate the physical parameters from online measurements. The main advantage of this category is that it yields the physical parameters. Each parameter has its physical meaning, which sounds good especially for power engineers. Many different methods have been used for such a purpose. Singular value decomposition (SVD) [9], subspace identification methods [10], neural networks [11], extended Kalman filter [12], conjugate gradient method [13], maximum likelihood [14], evolutionary programming [15], orthogonal series functions [16], and Hartley series [17] are among the methods used for identification of parameters of a synchronous generator.

Along with the identification strategy, papers differ in the model structure and the kind of system disturbance during measurements. The conventional online tests for machine modeling involve large disturbances, such as load rejection and three-

Manuscript received September 4, 2002.

M. Karrari is with the Department of Electrical Engineering, Amirkabir University of Technology, Tehran, Iran, on leave from the Department of Electrical and Computer Engineering, University of Calgary, Calgary, AB T2N 1N4, Canada (e-mail: karrari@ucalgary.ca).

O. P. Malik is with the Department of Electrical and Computer Engineering, University of Calgary, Calgary, AB T2N 1N4, Canada (e-mail: malik@enel.ucalgary.ca).

Digital Object Identifier 10.1109/TEC.2003.822296

phase short circuit [18]. However some approaches are based on small-disturbance responses such that it would not interfere with normal operating conditions [19], [20].

Depending on the desires and aim of the user, the model structure of a synchronous generator can significantly change. Synchronous generators are usually connected in a network. If the parameters of a synchronous generator are required for investigating the stability and oscillation of an overall multi-machine system, a third order model structure is adequate. Nevertheless the nonlinearities are very important, since the operating conditions of the synchronous generators vary considerably due to load demand changes.

In this paper, a third order nonlinear model is identified for a synchronous generator. The method used in this paper, identifies the physical parameters of the nonlinear structure using online measurements and has these features:

- a) It uses Heffron-Phillips model, as an intermediate step to derive the nonlinear model of a synchronous generator. All formulas are well-known and easy to derive. The mechanical parameters (i.e., rotor inertia and damping factor) as well as the electrical parameters are estimated.
- b) It requires only the electrical power and the terminal voltage as the outputs of the system with small perturbation of the field voltage.
- c) The unstructured nonlinearities are reflected in the changes in the parameters of the nonlinear structure.
- d) It requires the rotor angle to be measured only at steady-state conditions. Noise can significantly affect the accuracy of the measurement. This accuracy can be much improved by averaging the measurement over a long period of time. This is not possible if the rotor angle is required to be measured at each sampling instant, as required by the similar published approaches [10], [13] to calculate direct and quadratic variables at each sampling instant.
- e) Although the derived model is a third order model, it includes all structured nonlinearities. For highest accuracy, usually an 8th order model is considered. The derivation of the whole set of parameters for such a detailed model, involves extensive calculations. In [13] a vector of 61 parameters is estimated, each of which has a complicated nonlinear relation with the physical parameters. However, in a noisy environment, when the number of required parameters is increased, the set of acceptable parameters, from transfer function point of view, is wider [21], [22]. Therefore, determination of the exact values of the physical parameters is much more difficult and inaccurate. For a third order model, however, the number of required parameters is dramatically reduced. Therefore the effects of noise and the variance of the estimated parameters are effectively reduced.

The paper is organized as follows:

In Section 2, the proposed method is outlined. The nonlinear model structure considered for the simulation and modeling of the synchronous generator is explained in Section 3. The linearized model is also described. This linear model is used in an intermediate step to extract the physical parameters.

Extracting physical parameters from the estimated linear model is addressed in Section 4. In Section 5, the application of the proposed method on a micromachine is carried out and the experimental data is compared with the simulated nonlinear model of the synchronous generator. Section 6 concludes the paper.

II. PROPOSED METHOD

The method proposed in this paper is based on the fact that a well-defined linear and nonlinear structure is defined for the system. The linear structure is used as an intermediate step to extract the parameters of the nonlinear structure. To identify the parameters of the nonlinear structure, first a particular operating condition is selected. It is clear that the parameters of the linear transfer function would depend on the operating conditions and the physical parameters. The idea is to first identify the linear model (Heffron-Phillips model), then extract the physical parameters using the identified linear model. The nonlinear model is next simulated using the estimated physical parameters. The procedure is outlined below:

- 1) A particular operating condition is selected (e.g., nominal operating condition). The rotor angle at this operating condition is measured.
- 2) An exciting input signal is applied to the field of the synchronous generator. This input signal is added to the normal values. It should have enough frequency spectrum to excite the various modes of the system and the magnitude should be small, such that it would not interfere with the normal operation of the system. A pseudo random binary sequence (PRBS) with 5% of the nominal value is an appropriate input signal.
- 3) The applied input signal along with the terminal voltage and electrical power are sampled using a data acquisition system (DAS).
- 4) A multivariable linear transfer function is obtained for the system using the well-known identification methods for linear time-invariant systems (e.g., maximum likelihood).
- 5) Parameters of the identified transfer function are converted to the parameters of the Heffron-Phillips structure.
- 6) Physical parameters of the synchronous generator are extracted from the parameters of the Heffron-Phillips model.
- 7) The nonlinear structure is simulated with the estimated physical parameters.
- 8) The nonlinear model is used in some different operating conditions. At dramatically different operating conditions, the parameters of the nonlinear structure are adjusted for a better performance.

In this algorithm, steps 5 and 6 are the main steps. These two steps are explained in Section 4 in more detail. First the structure of the nonlinear and linear model is described in Section 3.

III. SYNCHRONOUS GENERATOR MODEL

In this study, a third order nonlinear structure has been adopted. Compared with higher order nonlinear structures, it

neglects the effects of damper windings and dynamics of the stator. These two effects can be neglected, especially when the very fast dynamics (sub-transients) are not of interest. The effect of damper windings is approximately considered in the rotor damping factor. A synchronous machine connected to infinite bus through a transmission line, Fig. 1, is considered here as the study system.

The third order nonlinear structure derived in [23], [24] is used in this study. The only modification is that the parameters and the variables of the model are not in per unit. The model then is described by these equations:

$$\begin{aligned}\dot{\delta} &= \omega \\ \dot{\omega} &= \frac{1}{J}(T_m - T_e - D \cdot \omega) \\ \dot{e}'_q &= \frac{1}{T_{d0}'}(E_{FD} - e'_q - (x_d - x'_d) \cdot i_d)\end{aligned}\quad (1)$$

where:

$$\begin{aligned}T_e &= \frac{v_d \cdot i_d + v_q \cdot i_q}{\omega} \cong \frac{v_d \cdot i_d + v_q \cdot i_q}{\omega_0} \\ i_d &= \frac{e'_q - v_q}{x'_d}, i_q = \frac{v_d}{x_q}\end{aligned}$$

Other variables and the constants are defined in Appendix A.

The linearized form of the above model is:

$$\begin{aligned}\Delta \dot{\delta} &= \Delta \omega \\ \Delta \dot{\omega} &= \frac{1}{J}(\Delta T_m - K_1 \Delta \delta - K_2 \Delta e'_q - D \cdot \Delta \omega) \\ \Delta \dot{e}'_q &= \frac{K_3}{T_f}(\Delta E_{FD} - K_4 \Delta \delta - \Delta e'_q)\end{aligned}\quad (2)$$

In (2), K_1, K_2, K_3, K_4 , and T_f are constants depending on system parameters and the operating conditions (explained in Appendix A). This model, known as the Heffron-Phillips model, is used in an intermediate step to extract the physical parameters (x_d, x'_d, \dots) from the identified model. This linear model can be described in state space and transfer function structures as given in Appendix A.

IV. EXTRACTION OF PHYSICAL PARAMETERS

Although the linear system described in Appendix A, is a two input, two output system, to make it more practical, only the field voltage is considered as the input, because the field voltage is an electric signal and can be disturbed and measured more easily than the mechanical torque.

Assuming that the transfer function between the outputs ($y_1 =$ electrical power, $y_2 =$ terminal voltage) and the input ($u_1 =$ field voltage) is known, a procedure to extract physical parameters is outlined here. Suppose the identified transfer functions are:

$$\begin{aligned}G_{11}(s) &= \frac{y_1(s)}{u_1(s)} = \frac{N_{11}(s)}{\Delta(s)} = \frac{a_{11}^2 s^2 + a_{11}^1 s}{s^3 + a_0^2 s^2 + a_0^1 s + a_0^0} \\ G_{21}(s) &= \frac{y_2(s)}{u_1(s)} = \frac{N_{21}(s)}{\Delta(s)} = \frac{a_{21}^2 s^2 + a_{21}^1 s + a_{21}^0}{s^3 + a_0^2 s^2 + a_0^1 s + a_0^0}\end{aligned}\quad (3)$$

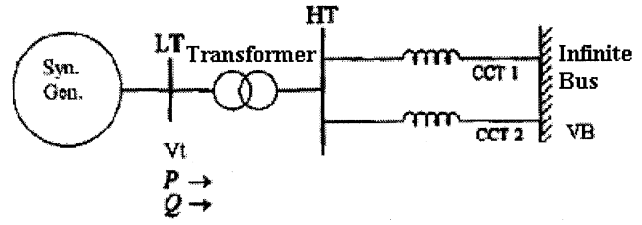


Fig. 1. Structure of the study system.

It is shown in Appendix A, that:

$$\begin{aligned}a_0^2 &= \frac{D}{J} + \frac{1}{T_f}, \quad a_0^1 = \frac{D}{JT_f} + \frac{K_1}{J}, \\ a_0^0 &= \frac{K_1}{JT_f} - \frac{K_2 K_3 K_4}{JT_f}, \\ a_{11}^2 &= \frac{K_2 K_3}{T_f}, \quad a_{11}^1 = \frac{K_2 K_3 D}{JT_f}, \\ a_{21}^2 &= \frac{K_6 K_3}{JT_f}, \quad a_{21}^1 = \frac{K_6 K_3 D}{JT_f}, \\ a_{21}^0 &= \frac{K_1 K_3 K_6 - K_2 K_3 K_5}{JT_f}\end{aligned}\quad (4)$$

Having identified the ' a ' parameters and using (4), one can calculate:

$$\begin{aligned}\frac{D}{J} &= \frac{a_{11}^1}{a_{11}^2} \quad K_6 \cdot K_3 = a_{21}^2 \times T_f \\ T_f &= \frac{1}{a_0^2 - \frac{a_{11}^1}{a_{11}^2}} \quad \frac{K_4}{J} = \frac{\frac{K_1}{J} - a_0^0 \times T_f}{K_2 \cdot K_3} \\ \frac{K_1}{J} &= a_0^1 - \frac{D}{J} \cdot \frac{1}{T_f} \quad \frac{K_5}{J} = \frac{\frac{K_1}{J} \cdot K_3 \cdot K_6 - a_{21}^0 \times T_f}{K_2 \cdot K_3} \\ K_2 \cdot K_3 &= a_{11}^2 \times T_f\end{aligned}\quad (5)$$

Comparing the parameters obtained in (5) from the transfer functions with the parameters of the Heffron-Phillips model, it is clear that not all the parameters of the Heffron-Phillips model can be calculated from the identified transfer functions. For example, although the values of $K_2 K_3$ and $K_2 K_6$ have been identified, there is no unique value for K_2, K_3 , and K_6 . Although the whole set of parameters for the Heffron-Phillips model has not been identified, enough values are known to calculate the physical parameters of the nonlinear structure, which are $x_d, x_q, x'_d, x_e, T'_{d0}, J$, and D . Suppose P, Q, v_{t0} and the rotor angle (δ_0) have been measured. Then i_{d0}, i_{q0}, v_{d0} , and v_{q0} can be calculated using (1).

Now, x_d, x_q, x'_d, x_e , and J can be calculated from the following set of nonlinear algebraic equations (the line and transformer resistance r_e can be considered as zero or, for higher accuracy, should be estimated separately using some steady-state measurements).

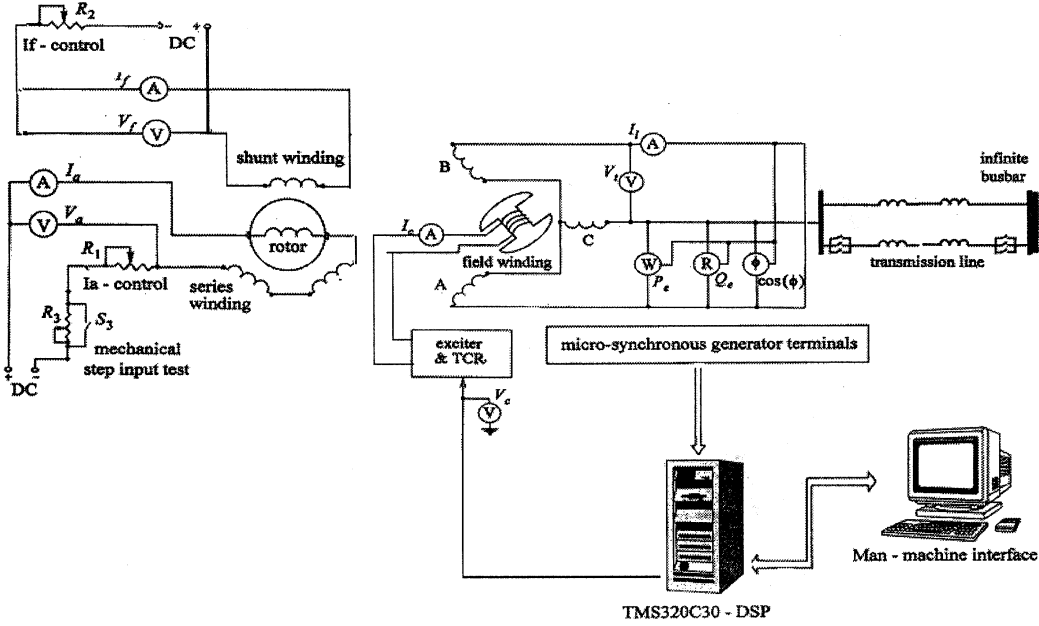


Fig. 2. Experimental setup for the micromachine.

$$\begin{aligned}
 \frac{K_1}{J} &= \frac{f_d}{J\omega_0} \cdot (x_q - x'_d) \cdot i_{q0} + \frac{f_q}{J\omega_0} \cdot (v_{q0} + x_q \cdot i_{d0}) \\
 K_2 K_3 &= \left(\frac{i_{q0}}{\omega_0} + \frac{y_d}{\omega_0} \cdot (x_q - x'_d) \cdot i_{q0} \right. \\
 &\quad \left. + \frac{y_q}{\omega_0} \cdot (v_{q0} + x_q \cdot i_{d0}) \cdot \left(\frac{1}{1 + (x_d - x'_d) \cdot y_d} \right) \right) \\
 K_3 K_6 &= \left(\frac{v_{q0}}{v_{t0}} + y_d \cdot \frac{-x'_d \cdot v_{q0}}{v_{t0}} + y_q \cdot \frac{x_q \cdot v_{d0}}{v_{t0}} \right) \\
 &\quad \cdot \left(\frac{1}{1 + (x_d - x'_d) \cdot y_d} \right) \\
 \frac{K_4}{J} &= \frac{f_d}{J} \cdot (x_d - x'_d) \\
 \frac{K_5}{J} &= \frac{f_d}{J} \cdot \frac{-x'_d \cdot v_{q0}}{v_{t0}} + \frac{f_q}{J} \cdot \frac{x_q \cdot v_{d0}}{v_{t0}}
 \end{aligned} \tag{6}$$

This nonlinear set of equations can be solved using any of the well-known numerical approaches like Newton-Raphson method (using MATLAB software).

Once these variables are calculated, one can calculate:

$$\begin{aligned}
 K_3 &= \frac{1}{1 + (x_d - x'_d) \cdot \frac{x_e + x_q}{r_e^2 + (x_e + x_q)(x_e + x'_d)}} \\
 T'_{d0} &= \frac{T_f}{K_3} \\
 D &= \frac{D}{J} \times J
 \end{aligned} \tag{7}$$

Now, the remaining parameters of the Heffron-Philips model (K_2, K_6) can be calculated, if necessary, though they are not required. The algorithm described in this section to extract physical parameters of a synchronous generator is an easy algorithm

to implement compared to other algorithms developed in the literature. It only requires an online experiment with the generator in normal operation in which the field voltage is disturbed by an exciting signal with small magnitude. The defined output signals are easily measurable.

V. IMPLEMENTATION OF THE PROPOSED METHOD ON A MICROMACHINE

In this section, implementation of the proposed method on a micromachine is described.

A. Experimental Setup and Results

The system under consideration is a 3-kVA micromachine, driven by a dc motor. The micromachine can represent dynamic response of much larger machines, when the parameters and variables are considered in a normalized version (per unit system [23]). The main problem with a micromachine can be the field time constant, which is much lower than that of the larger machines. This problem has been overcome using a time constant regulator, which is used to increase the effective field time constant to match that of the larger units.

The transmission line is modeled by a lumped element transmission line. It consists of six π sections and simulates the performance of a 300 km long 500 kV, double circuit transmission line connected to a constant voltage bus.

The experimental setup used for the experiment is shown in Fig. 2. The synchronous generator is driven by a DC motor. The exciting input signal, PRBS, with a magnitude of 5% of the field voltage nominal value, is produced in the computer and is applied to the synchronous machine through a D/A converter. The field voltage, terminal voltage and the electrical power are measured and sampled by the data acquisition system.

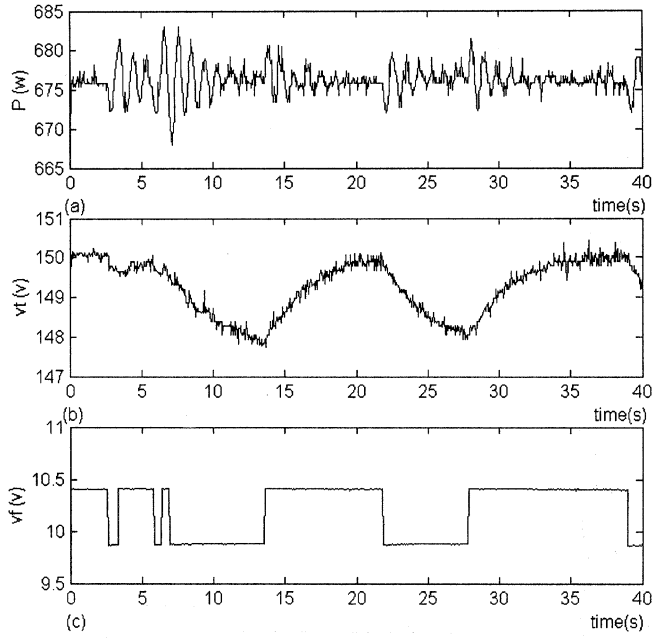


Fig. 3. Experimental results.

One important requirement of the proposed method is the rotor angle measurement. This is accomplished by comparing two pulse trains, one obtained from the frequency of the terminal voltage (zero crossing) and the other obtained from a signal from the rotor. A disk with four holes is installed on the rotor and a photo diode produces four pulses each revolution. Details of such a measurement can be found in [25].

The main operating condition was selected to be $P = 675$ W (per phase), $Q = 0$ and $v_{t0} = 150$ V. The rotor angle and the field voltage at this operating condition were measured as: $\delta = 34.6$ degrees and $v_f = 10.4$ V.

The sampling time was selected to be 50 ms. This sampling time proved to be fast enough to capture the required dynamics. The line resistance was estimated to be $r_e = 1.15 \Omega$. Fig. 3 shows the field voltage, terminal voltage and the electrical power measured from the experiment at the main operating conditions. These results are used in the next section to identify the system. The spikes in the measurement results are because of the measurement noise and the data degradation caused by the data acquisition system.

B. System Identification

Identification of linear time invariant systems is well established in the literature and much software has been developed for such a procedure. In this work, the programs in MATLAB were used to identify the system. Recursive Extended Least Square (RELS), Recursive Instrumental Variable (RIV) and Prediction Error Method (PEM) resulted in a very similar set of parameters. The degree of the numerator, the degree of the denominator and the delay should be selected such that the required transfer function with structure described in Appendix A, is obtained. The transfer functions are first identified in discrete

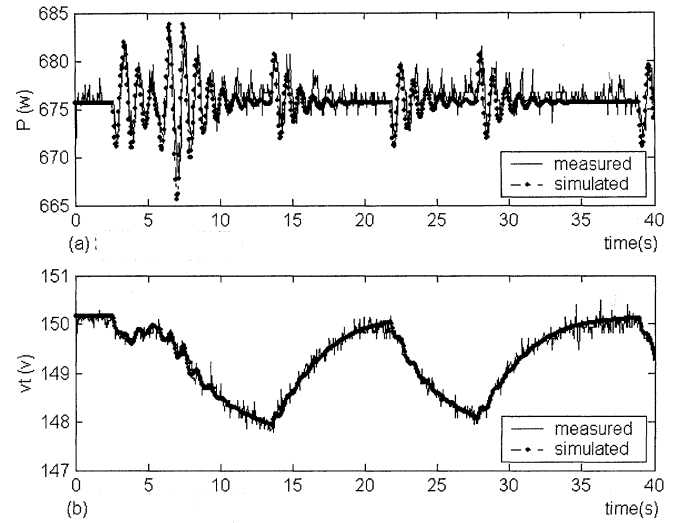


Fig. 4. Outputs of the experimental results and the identified transfer functions.

time form and then transferred to continuous domain. The final transfer functions are:

$$\frac{N_{11}(s)}{\Delta(s)} = \frac{0.0093 s^2 + 0.001 s}{s^3 + 1.5713 s^2 + 44.3881 s + 18.1129}$$

$$\frac{N_{21}(s)}{\Delta(s)} = \frac{0.1812 s^2 + 0.0196 s + 3.952}{s^3 + 1.5713 s^2 + 44.3881 s + 18.11291}$$

A comparison of the experimental results with the outputs of the identified transfer functions is given in Fig. 4, which shows fairly accurate identification.

C. Extraction of the Physical Parameters

In this section, the equations derived in Section 4 are used to extract the physical parameters of the synchronous generator. From the identified transfer function (comparing the identified transfer function and those obtained in Appendix A and (4)), gives:

$$a_0^2 = 1.5713, \quad a_0^1 = 44.3881, \quad a_0^0 = 18.112,$$

$$a_{11}^2 = 0.0093, \quad a_{11}^1 = 0.001,$$

$$a_{21}^2 = 0.1812, \quad a_{21}^1 = 0.0196, \quad a_{21}^0 = 3.952$$

Then using (5):

$$\frac{D}{J} = \frac{a_{11}^1}{a_{11}^2} = \frac{0.001}{0.0093} = 0.108$$

$$T_f = \frac{1}{a_0^2 - \frac{a_{11}^1}{a_{21}^2}} = \frac{1}{1.5713 - 0.108} = 0.6834$$

$$\frac{K_1}{J} = a_0^1 - \frac{D}{J} \cdot \frac{1}{T_f} = 44.3881 - 0.108/0.6834 = 44.23$$

$$K_2 \cdot K_3 = a_{11}^2 \times T_f = 0.0093 \times 0.688 = 0.0064$$

$$K_6 \cdot K_3 = a_{21}^2 \times T_f = 0.1812 \times 0.6834 = 0.1238$$

$$\frac{K_4}{J} = \frac{K_1}{K_2 \cdot K_3} - a_0^0 \times T_f = \frac{44.23}{0.0064} - 18.112 \times 0.6834 = 4986$$

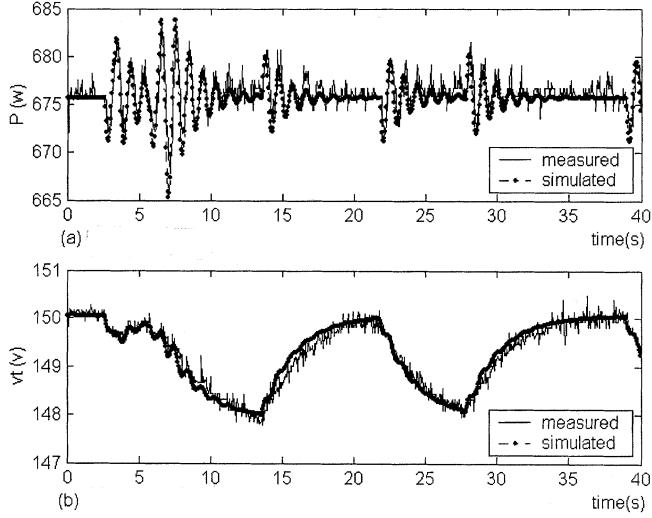


Fig. 5. Outputs of the experimental results and of the identified nonlinear model.

$$\begin{aligned} \frac{K_5}{J} &= \frac{K_1 \cdot K_3 \cdot K_6 - a_{21}^0 \times T_f}{K_2 \cdot K_3} \\ &= \frac{44.23 \times 0.1238 - 3.952 \times 0.6834}{0.0064} = 434.5 \end{aligned}$$

Having measured $P = 675$ W, $Q = 0$, $v_{t0} = 150$ V, and $\delta = 34.6^\circ$, and using (1), gives:

$$\begin{aligned} i &= \frac{P^2 + Q^2}{v_{t0}} = 4.6587 \text{ A} \\ \varphi &= tg^{-1} \frac{Q}{P} = 0 \\ v_{d0} &= v_{t0} \cdot \sin \delta_0 = 85.2066 \text{ V} \\ v_{q0} &= v_{t0} \cdot \cos \delta_0 = 123.5188 \text{ V} \\ i_{d0} &= i \cdot \sin(\delta_0 + \varphi) = 3.54 \text{ A} \\ i_{q0} &= i \cdot \cos(\delta_0 + \varphi) = 3.0286 \text{ A} \\ v_{bd} &= v_d - r_e i_d + x_e i_q = 100.2159 \text{ V} \\ v_{bq} &= v_q - r_e i_q - x_e i_d = 97.7341 \text{ V} \\ v_B &= \sqrt{v_{bd}^2 + v_{bq}^2} = 139.9828 \text{ V} \end{aligned}$$

Now using (6) and solving the set of nonlinear equations gives:

$$\begin{aligned} x_d &= 40.1098 \Omega \\ x_q &= 28.134 \Omega \\ x'_d &= 0.01 \Omega \\ x_e &= 6.3 \Omega \\ J &= 0.1228 \text{ kg}\cdot\text{m}^2 \end{aligned}$$

Using (7):

$$\begin{aligned} K_3 &= 0.1367 \\ T'_d \sigma &= 5.0 \text{ s} \\ D &= 0.0133 \text{ N}\cdot\text{m}\cdot\text{s} \end{aligned}$$

Thus the whole set of parameters for the nonlinear model is calculated. In the next section, this model is evaluated.

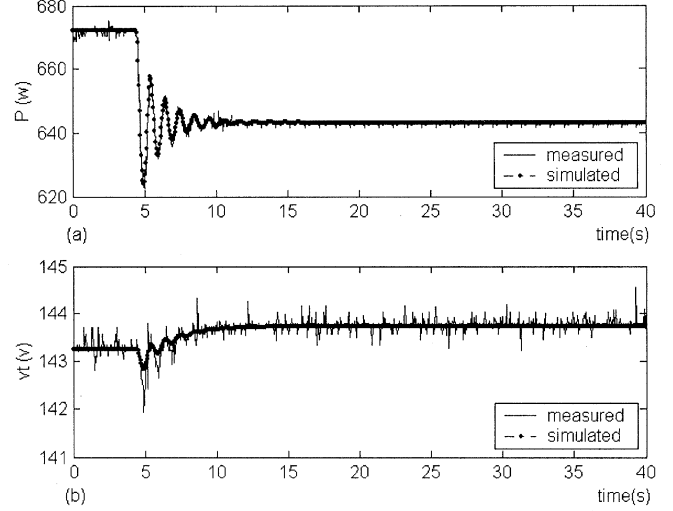


Fig. 6. Outputs of the experimental results and of the identified nonlinear model following a mechanical step change.

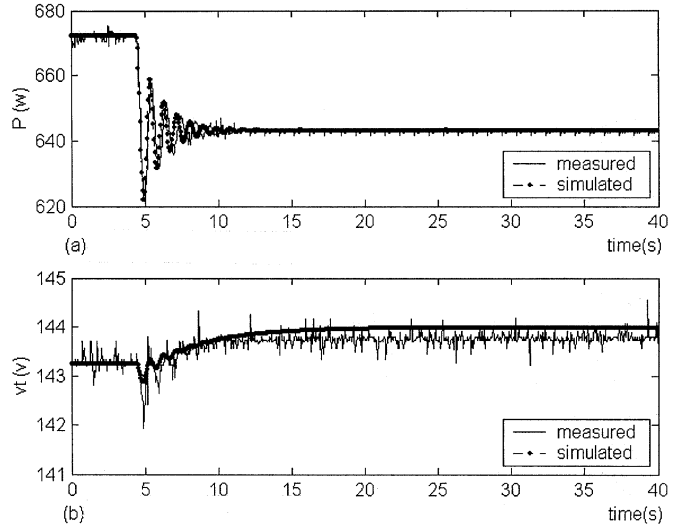


Fig. 7. Outputs of the experimental results and of the identified linear model following a mechanical step change.

D. Model Validation

A comparison of the experimental data with the output of the nonlinear model obtained in the previous section is shown in Fig. 5. Comparing Figs. 4 and 5, it is seen that the linear model fits the measured data slightly better than the nonlinear model. However, the advantage of the nonlinear model over the linear model would become clear when the operating condition of the system is changed from the one at which the linear model has been identified.

Response of the system and the nonlinear model following a step change in the mechanical input and the field voltage showed an acceptable performance of the nonlinear system. Fig. 6 compares the experimental results and of the identified nonlinear model following a 21.75% mechanical step change.

The identified linear model (as could have been predicted) can not follow the step changes properly, as shown in Fig. 7. Response of the system and the nonlinear model following a

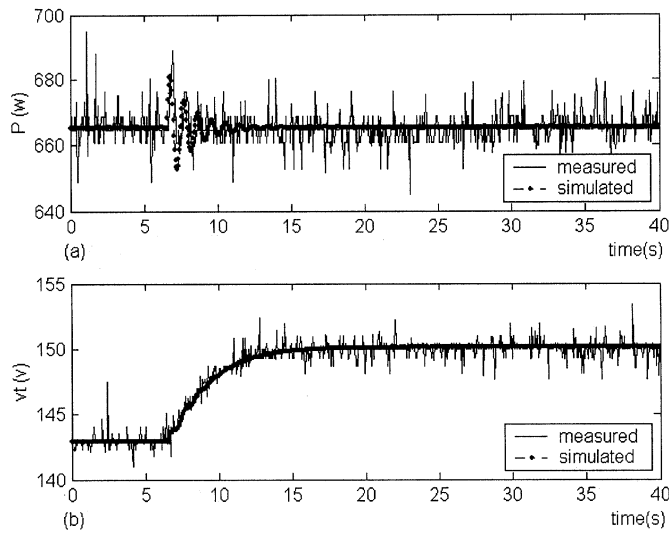


Fig. 8. Outputs of the experimental results and of the identified nonlinear model following a field voltage step change.

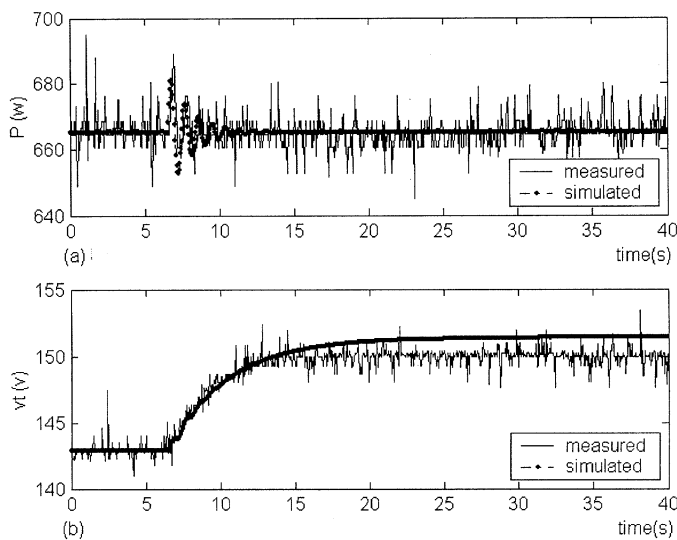


Fig. 9. Outputs of the experimental results and of the identified linear model following a field voltage step change.

step change in the field voltage, is given in Fig. 8. Response of the system and the linear model following the same step change is shown in Fig. 9.

Additional experimental and simulation results (not shown for the sake of brevity) yielded the same conclusion. The linear model not only shows steady-state error in all state variables (the steady-state error is not present in the electrical power, since the transfer function is unity at steady state, regardless of the parameters of the system), but also do not follow the oscillations properly. The nonlinear model, however, shows a good performance at other operating conditions, with no steady-state error and good match during transients.

Although the model, derived in the previous sections is a nonlinear model and performs much better than the linear model when the operating conditions of the system change, even the nonlinear model would degrade when the operating conditions

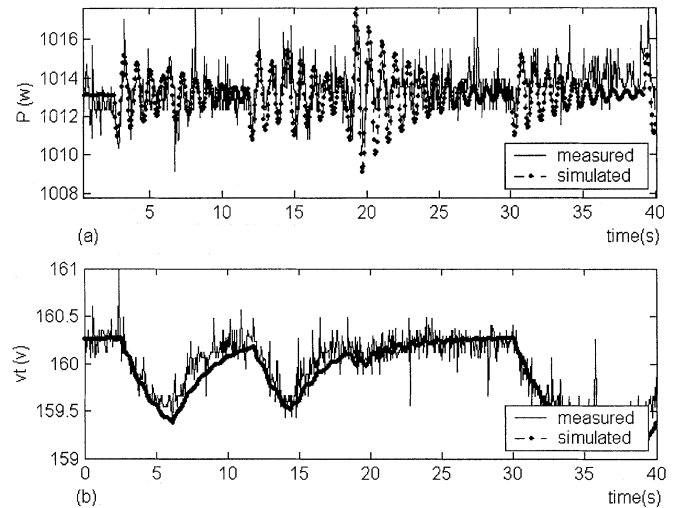


Fig. 10. Outputs of the experimental results at $P = 1013$ W and $Q = 400$ VAR and of the identified nonlinear model identified at $P = 675$ and $Q = 0$.

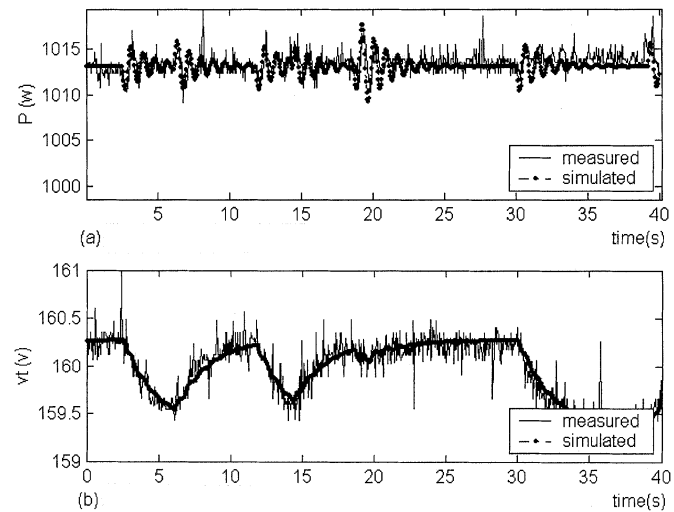


Fig. 11. Outputs of the experimental results at $P = 1013$ W and $Q = 400$ VAR and of the identified nonlinear model identified at the same operating conditions.

of the system change dramatically. A comparison of the experimental data with the output of the nonlinear model obtained in the previous section at a very different operating condition is shown in Fig. 10. For this experiment the operating condition was selected to be $P = 1013$ W (per phase), $Q = 400$ VAR and $v_{f0} = 160$ V. As it can be seen from the figure, the model has, to some extent, degraded.

Although the model degradation may be acceptable for some applications, especially controller design, the model can be improved by considering the parameters of the nonlinear structure as dependent on the operating conditions.

Fig. 11 shows the same results with a new set of identified model for this particular operating conditions. For the new operating conditions, $x_d = 38.1 \Omega$, $x_q = 26.0 \Omega$ were identified. The rest of the parameters remained approximately the same as before. Some other tests were carried out at another operating condition $P = 400$ W (per phase), $Q = -160$ VAR and

$v_{t0} = 133$ V. The same conclusion was reached. The comparison is not given for the sake of brevity. For this particular operating condition, $x_d = 43.1 \Omega$, $x_q = 29.0 \Omega$ were estimated. As the results show, x_d and x_q are the main parameters which change with the operating conditions. The main reason for such variations is the magnetic saturation in the iron parts of the rotor and stator, as stated in the Introduction.

VI. CONCLUSION

A new method for the identification of the physical parameters of a synchronous generator is presented in this paper. The method is based on the fact that for the synchronous generator well-defined linear and nonlinear model structures exist. The Heffron-Phillips model is used to extract physical parameters from the identified transfer functions. The proposed method requires very simple test on the machine during normal operation.

Experimental results show that machine performance using the obtained parameters in the standard two-axis model of the machine match fairly closely the actual performance of the physical machine, especially when the operating condition of the system is changed.

The obtained model was also tested at dramatically different operating conditions. The model shows fairly good accuracy for those operating conditions as well. To improve the performance of the model, the direct and quadratic axes reactances can be adjusted slightly.

APPENDIX A

The main variables and constants of (1) are:

$$\begin{aligned} i &= \frac{P^2 + Q^2}{v_t}, \quad \varphi = \tan^{-1} \frac{Q}{P} \\ v_d &= v_t \cdot \sin \delta, \quad v_q = v_t \cdot \cos \delta \\ i_d &= i \cdot \sin(\delta + \varphi), \quad i_q = i \cdot \cos(\delta + \varphi) \\ v_{bd} &= v_d - r_e i_d + x_e i_q, \quad v_{bq} = v_q - r_e i_q - x_e i_d \\ v_B &= \sqrt{v_{bd}^2 + v_{bq}^2} \\ x_d &= x_{ad} + x_l, \quad x_q = x_{aq} + x_l \end{aligned}$$

J, D	rotor inertia and damping factor;
T_{d0}'	direct-axis transient time constant;
x_l	stator leakage reactance;
x_{ad}, x_{aq}	direct and quadratic axis mutual reactance;
x_d'	direct transient reactance;
x_e, r_e	line and transformer reactance and resistance;
δ	rotor angle;
ω	rotor speed;
T_m	mechanical input torque;
E_{FD}	steady-state internal voltage of armature;
e_q'	transient internal voltage of armature;
P, Q	terminal active and reactive power per phase;
v_t	terminal voltage;
v_B	infinite bus voltage.

The constants of the linear model are

$$\begin{aligned} K_1 &= \frac{f_d}{\omega_0} \cdot (x_q - x_d') \cdot i_{q0} + \frac{f_q}{\omega_0} \cdot (v_{q0} + x_q \cdot i_{d0}) \\ K_2 &= \frac{i_{q0}}{\omega_0} + \frac{y_d}{\omega_0} \cdot (x_q - x_d') \cdot i_{q0} + \frac{y_q}{\omega_0} \cdot (v_{q0} + x_q \cdot i_{d0}) \\ K_3 &= \frac{1}{1 + (x_d - x_d') \cdot y_d} \\ K_4 &= f_d \cdot (x_d - x_d') \\ T_f &= K_3 \cdot T_{do}' \end{aligned}$$

where

$$\begin{aligned} f_d &= \frac{v_B}{z_e^2} \cdot (-r_e \cdot \cos \delta_0 + x_1 \cdot \sin \delta_0) \\ f_q &= \frac{v_B}{z_e^2} \cdot (r_e \cdot \sin \delta_0 + x_2 \cdot \cos \delta_0) \\ y_d &= \frac{x_1}{z_e^2}, \quad y_q = \frac{r_e}{z_e^2} \\ z_e^2 &= r_e^2 + x_1 \cdot x_2 \\ x_1 &= x_e + x_q, \quad x_2 = x_e + x_d' \end{aligned}$$

In the above equations, subscript "0" stands for the values of the variables at the operating point at which the model is linearized. Details of the derivation of these constants can be found in [22], [23].

To represent the linear model described in Section 3 in state space form, the states, inputs and outputs should be defined. The states and inputs are defined as follows:

$$\underline{x} = \begin{bmatrix} x_1 \\ x_2 \\ x_3 \end{bmatrix} = \begin{bmatrix} \Delta \delta \\ \Delta \omega \\ \Delta e_q' \end{bmatrix}, \quad \underline{u} = \begin{bmatrix} u_1 \\ u_2 \end{bmatrix} = \begin{bmatrix} \Delta E_{FD} \\ \Delta T_M \end{bmatrix}.$$

Definition of the outputs is slightly arbitrary. Considering practical aspects, in this study, ΔP_e , active output power deviation per phase and Δv_t , terminal voltage deviation were considered as the outputs. Using these definitions the state space model of the system is [22], [23]

$$\begin{aligned} \dot{\underline{x}} &= A \underline{x} + B \underline{u} \\ \underline{y} &= C \underline{x} \end{aligned}$$

where

$$\begin{aligned} A &= \begin{bmatrix} 0 & 1 & 0 \\ -\frac{K_1}{J} & -\frac{D}{J} & -\frac{K_2}{J} \\ -\frac{K_2 K_3}{T_f} & -\frac{1}{T_f} & 0 \end{bmatrix}, \quad B = \begin{bmatrix} 0 & 0 \\ 0 & -\frac{1}{J} \\ \frac{K_3}{T_f} & 0 \end{bmatrix} \\ C &= \begin{bmatrix} K_1 & 0 & K_2 \\ K_5 & 0 & K_6 \end{bmatrix} \end{aligned}$$

and K_5 and K_6 can be calculated by

$$\begin{aligned} K_5 &= f_d \cdot \frac{-x_d' \cdot v_{q0}}{v_{t0}} + f_q \cdot \frac{x_q \cdot v_{d0}}{v_{t0}} \\ K_6 &= \frac{v_{q0}}{v_{t0}} + y_d \cdot \frac{-x_d' \cdot v_{q0}}{v_{t0}} + y_q \cdot \frac{x_q \cdot v_{d0}}{v_{t0}} \end{aligned}$$

This model can also be shown in transfer function structure. The transfer function $G(s)$ can be obtained using the equation

$$G(s) = C(sI - A)^{-1}B \Rightarrow \begin{bmatrix} Y_1(s) \\ Y_2(s) \end{bmatrix} = \begin{bmatrix} G_{11}(s) & G_{12}(s) \\ G_{21}(s) & G_{22}(s) \end{bmatrix} \begin{bmatrix} U_1(s) \\ U_2(s) \end{bmatrix} \Rightarrow \begin{bmatrix} Y_1(s) \\ Y_2(s) \end{bmatrix} = \frac{1}{\Delta} \begin{bmatrix} N_{11}(s) & N_{12}(s) \\ N_{21}(s) & N_{22}(s) \end{bmatrix} \begin{bmatrix} U_1(s) \\ U_2(s) \end{bmatrix}.$$

Using A, B, and C of the state space model, one may obtain

$$\Delta = s^3 + \left(\frac{D}{J} + \frac{1}{T_f}\right)s^2 + \left(\frac{D}{JT_f} + \frac{K_1}{J}\right)s + \left(\frac{K_1}{JT_f} - \frac{K_2K_3K_4}{JT_f}\right)$$

$$N_{11}(s) = \frac{K_2K_3}{T_f}s^2 + \frac{K_2K_3D}{JT_f}s$$

$$N_{22}(s) = \frac{K_5}{J}s + \frac{K_5 - K_6K_3K_4}{JT_f}$$

$$N_{21}(s) = \frac{K_6K_3}{T_f}s^2 + \frac{K_6K_3D}{JT_f}s + \frac{K_1K_3K_6 - K_2K_3K_5}{JT_f}$$

$$N_{12}(s) = \frac{K_1}{J}s + \frac{K_1 - K_2K_3K_4}{JT_f}.$$

REFERENCES

- [1] L. A. Kilgore, "Calculation of synchronous machine constants," *AIEE Trans.*, vol. 50, pp. 1201–1214, Dec. 1931.
- [2] S. H. Wright, "Determination of synchronous machine constants by test," *AIEE Trans.*, vol. 50, pp. 1331–1351, Dec. 1931.
- [3] *Test Procedures for Synchronous Machines, Part I—Acceptance and Performance Testing, Part II—Test Procedures and Parameter Determination for Dynamic Analysis.*
- [4] A. M. El-Serafi and J. Wu, "Determination of the parameters representing the cross-magnetizing effect in saturated synchronous machines," *IEEE Trans. Energy Conversion*, vol. 8, pp. 333–340, Sept. 1993.
- [5] E. Levi and A. L. Viktor, "Impact of dynamic cross saturation on accuracy of saturated synchronous machine models," *IEEE Trans. Energy Conversion*, vol. 15, pp. 224–230, June 2000.
- [6] R. Warmkeue, N. E. E. Elkadri, I. Kamwa, and M. Chacha, "Unbalanced transient-based finite-element modeling of large generators," *J. Elect. Power Syst. Res.*, vol. 56, no. 3, pp. 205–210, Dec. 2000.
- [7] M. Karrari and M. B. Menhaj, "Application of different neural networks for identification of power systems," in *Proc. United Kingdom Automat. Contr. Conf.*, U.K., Sept. 4–7, 2000.
- [8] P. Shamsollahi and O. P. Malik, "On-line identification of synchronous generator using neural networks," in *Proc. Can. Conf. Elect. Comput. Eng.*, 1996, pp. 595–598.
- [9] T.-Z. Jiang, Y.-X. Chen, and D. Yi, "The SVD applied to the identification of the basic parameters of synchronous machine," *J. Changsha Univ. Elect. Power*, vol. 15, no. 1, pp. 56–58, Feb. 2000.
- [10] L. Guoxiu, F. Ming, and D. Liang, "State-space identification of synchronous machines," in *Proc. 31st Universities Power Eng. Conf.*, Iraklio, Greece, Sept. 1996, pp. 114–117.
- [11] S. Pillutla and A. Keyhani, "Neural network observers for on-line tracking of synchronous generator parameters," *IEEE Trans. Energy Conversion*, vol. 14, pp. 23–31, Mar. 1999.
- [12] M. Zhonggiang, Z. Chen, Z. Nan, J. Ma, J. Jin, G. Qi, and D. Meng, "Dynamic parameter identification of synchronous machines," in *Proc. Chinese Soc. Elect. Eng.*, vol. 18, 1998, pp. 100–105.
- [13] T. H. Chiang, T. C. Yung, C. Chung-Linad, and H. Chiung-Yi, "On-line measurement-based model parameter estimation for synchronous generators: Model development and identification scheme," *IEEE Trans. Energy Conversion*, vol. 9, pp. 330–336, June 1994.
- [14] R. Wamkeue, I. Kamwa, X. Dai-Do, and A. Keyhani, "Iteratively reweighted least square for maximum likelihood identification of synchronous machine parameters from on-line tests," *IEEE Trans. Energy Conversion*, vol. 14, pp. 159–166, June 1999.
- [15] J. T. Ma and Q. H. Wu, "Estimation of generator parameters using evolutionary programming," in *Proc. Int. Conf. Contr.*, U.K., 1994, pp. 1442–1447.
- [16] J. Melgoza, R. Jesus, G. T. Heydt, and A. Keyhani, "An algebraic approach for identifying operating point dependent parameters of synchronous machine using orthogonal series expansions," *IEEE Trans. Energy Conversion*, vol. 16, pp. 92–98, Mar. 2001.
- [17] J. J. R. Melgoza, G. T. Heydt, A. Keyhani, B. L. Agrawal, and D. Selin, "Synchronous machine parameter estimation using Hartley series," *IEEE Trans. Energy Conversion*, vol. 16, pp. 49–54, Mar. 2001.
- [18] C. C. Lee and T. T. Owen, "A weighted least squares parameters estimator for synchronous generator," *IEEE Trans. Power App. Syst.*, vol. PAS-96, pp. 97–101, Jan. 1977.
- [19] H. Tsai, A. Keyhani, J. Demcko, and R. G. Farmer, "On-line synchronous machine parameter estimation from small disturbance operating data," *IEEE Trans. Energy Conversion*, vol. 10, pp. 25–35, Mar. 1995.
- [20] G. Manchur, D. C. Lee, M. E. Coultres, J. D. A. Griffin, and W. Watson, "Generator models established by frequency response tests on a 555 MVA machine," *IEEE Trans. Power App. Syst.*, vol. PAS-91, pp. 2077–2084, Sept./Oct. 1972.
- [21] M. Burth, G. C. Verghese, and M. Velez-Reyes, "Subset selection for improved parameter estimation in on-line identification of a synchronous generator," *IEEE Trans. Power Syst.*, vol. 14, pp. 218–225, Feb. 1999.
- [22] S. Salman, K. S. Smith, and I. D. Stewart, "Measurement of synchronous machine parameters; A practical experience," in *Proc. Highlights Universities Power Eng. Conf.*, U.K., 1995, pp. 785–788.
- [23] Y.-N. Yu, *Electric Power System Dynamics*. New York: Academic Press, 1983.
- [24] P. Kundor, *Power System Stability and Control*. New York: McGraw-Hill, 1994.
- [25] D. W. Huber, "Real-time digital automatic voltage regulator for a generating unit," Ph.D. dissertation, Univ. Calgary, Calgary, AB, Canada, 1974.

Mehdi Karrari received the B.Sc. degree in power engineering from Amirkabir University (Tehran Polytechnic), Tehran, Iran, and the M.Sc. and D.I.C. degrees from Imperial College, London, U.K., in 1987. He received the Ph.D. degree from Sheffield University, Sheffield, U.K., in 1991.

Currently, he is an Associate Professor in the Control Engineering Group at Amirkabir University. Karrari is now spending a sabbatical in the Department of Electrical and Computer Engineering, University of Calgary, Calgary, AB, Canada.

Dr. Karrari is an active member in the Power Engineering Group, which has been known as "Dominant Group" in the country.

O. P. Malik (M'66-SM'69-F'87-LF'00) graduated in electrical engineering from Delhi Polytechnic, India, in 1952, and received the M.E. degree in electrical machine design from the University of Roorkee, India, in 1962. He received the Ph.D. degree from the University of London, London, U.K., and the D.I.C. from the Imperial College of Science and Technology, London, U.K., in 1965.

He became Professor at the University of Calgary in 1974 and is a faculty professor emeritus.

Dr. Malik is a Fellow of the Institution of Electrical Engineers (London).